# EARTH TIDES RECORDINGS COULD HELP TO REMOVE THE AMBIGUITY OF THE FAULT PLAN SOLUTION

NICOLETA CADICHEANU

*"Sabba S. Ştefănescu" Institute of Geodynamics of the Romanian Academy, 19-21, Jean-Louis Calderon St., Bucharest 37, 020032, Romania*

*Les enregistrements des marées terrestres pourraient aider à enlever l'ambiguïté de la solution du plan de faille*. Dans le cas d'un tremblement de terre, la solution du plan de faille consiste en deux plans perpendiculaires l'un à l'autre (un plan principal et un autre auxiliaire). Mais l'algorithme ne peut pas préciser quelle est la faille réelle. Des informations géologiques et géophysiques supplémentaires sont nécessaires pour enlever l'ambiguïté. Dans cette étude, nous voulons établir si les enregistrements des déformations lents de la croûte terrestre, principalement les marées terrestres, sont utiles dans notre approche. Nous avons utilisé les solutions du plan de faille des tremblements de terre de Vrancea avec magnitude Mw supérieure à 4 et les enregistrements gravimétriques et clinométriques des observatoires géodynamiques souterraines Crăciuneşti et Ursoiu, et de l'observatoire géodynamique Căldăruşani, au cours de la période 2006–2017. Les résultats sont préliminaires et tiennent compte de la réponse spécifique et les caractéristiques du chaque type de capteur.

*Key words:* earth tide, tiltmeter, fault solution ambiguity, Vrancea, geodynamic observatories.

## 1. INTRODUCTION

The focal mechanism solution (FMS) is the result of an analysis of wave generated by an earthquake and recorded by a number of seismic stations. FMS describes the deformation in the source region that generates the seismic waves. In the case of a fault-related event it refers to the orientation of the fault plane that slipped. The slip vector is also known as a fault-plane solution. The single fault plane solution may be modeled as a double couple (main plane and auxiliary plane). It is not possible to determine solely from a focal mechanism which of the nodal planes is in fact the fault plane. Additional geological and geophysical information is needed to remove ambiguity. In this study, we want to see if the slow crust deformation recordings, mainly the earthtides, are useful in this direction.

We considered that the clinometric records of the geodynamic observatories can provide important information about the slope of the fault plane and can contribute to solving, at least in the case of Vrancea intermediate earthquakes, the ambiguity of the normal and reverse fault planes. We analyzed intermediate earthquakes because in the case of normal earthquakes the movement propagates in a more complicated system of superficial faults implying a dynamics of the compartments that are harder to decipher.

## 2. METHOD AND DATA

Focal mechanisms are derived from a solution of the moment tensor for the earthquake, which itself is estimated by an analysis of observed seismic waveforms. The focal mechanism can be derived from observing the pattern of "first motions", that is, whether the first arriving P waves break up or down (Fig. 1).

The seismic waves radiated from an earthquake reflect the geometry of the fault and the motion on it. The geometry of a fault is described by: dip angle (δ), strike angle (φ) and slip angle (λ) (Fig. 2):

Seismologists use information from seismograms to calculate the FMS and typically display it on maps as a "beach ball" symbol. To obtain a beach ball representation, the data for an earthquake is plotted using a lower-hemisphere stereographic projection (Fig. 3).

For mechanisms calculated from first-motion directions of P-wave there is an ambiguity in identifying the fault plane on which slip occurred from the orthogonal, mathematically equivalent, auxiliary plane. We illustrate this ambiguity with four examples (Fig. 4). The block diagrams adjacent to each focal mechanism illustrate the two possible types of fault motion that the focal mechanism could represent. Note that the view angle is 30-degrees to the left of and above each diagram (USGS, 1996).

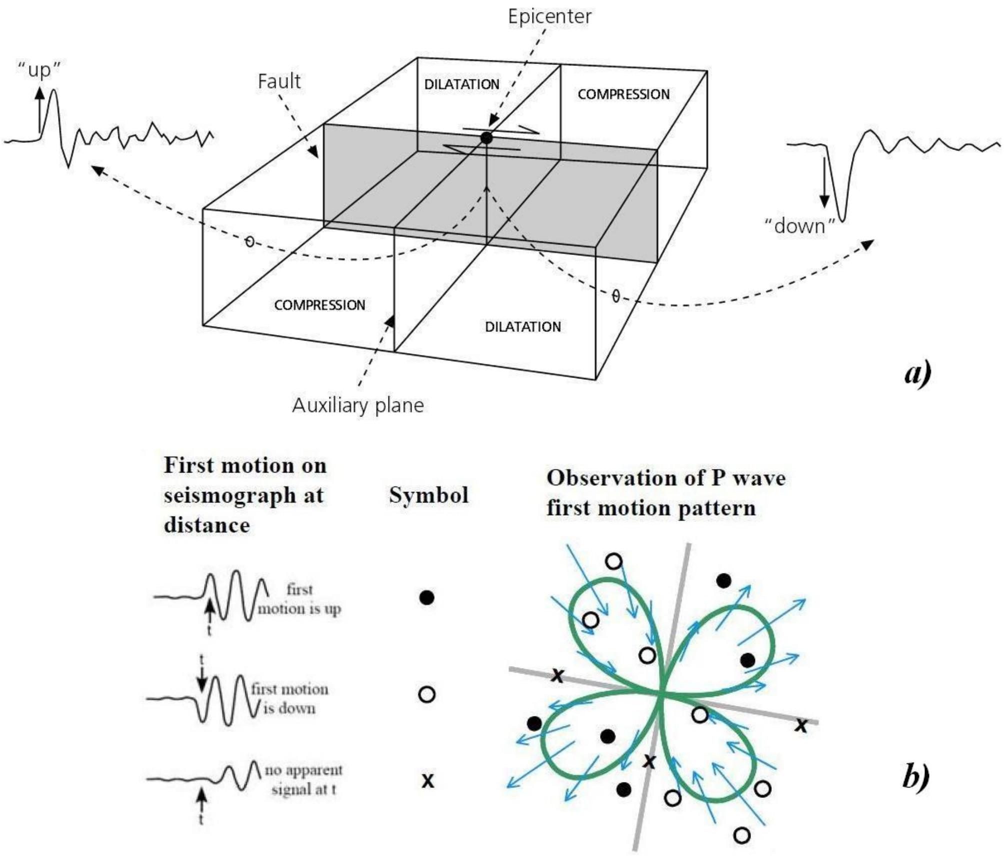


Fig. 1 – Nodal planes (a) (Bath, 1979) and the first motions of seismic P waves (b) (Stein, Wysession, 2003).

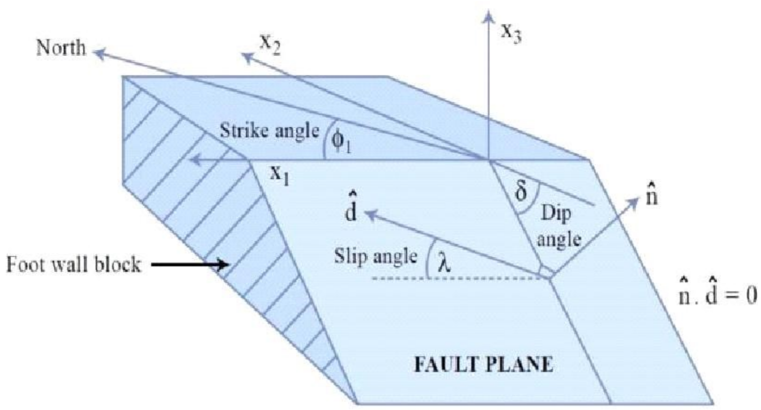


Fig. 2 – Geometry of the fault: the orientation of the fault determined by the direction of the fault, the inclination angle and the slip angle (Havskov, Ottemöller, 2010).

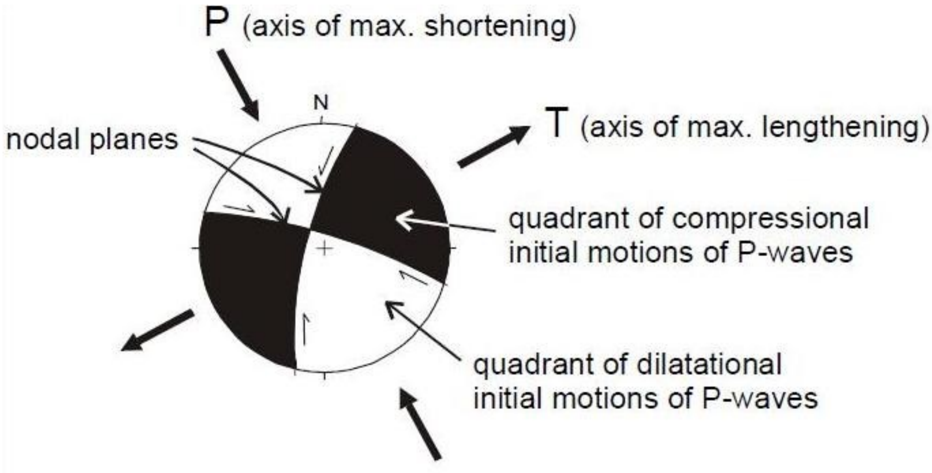


Fig. 3 – Stereographic projection of lower hemisphere (Bath, 1979).

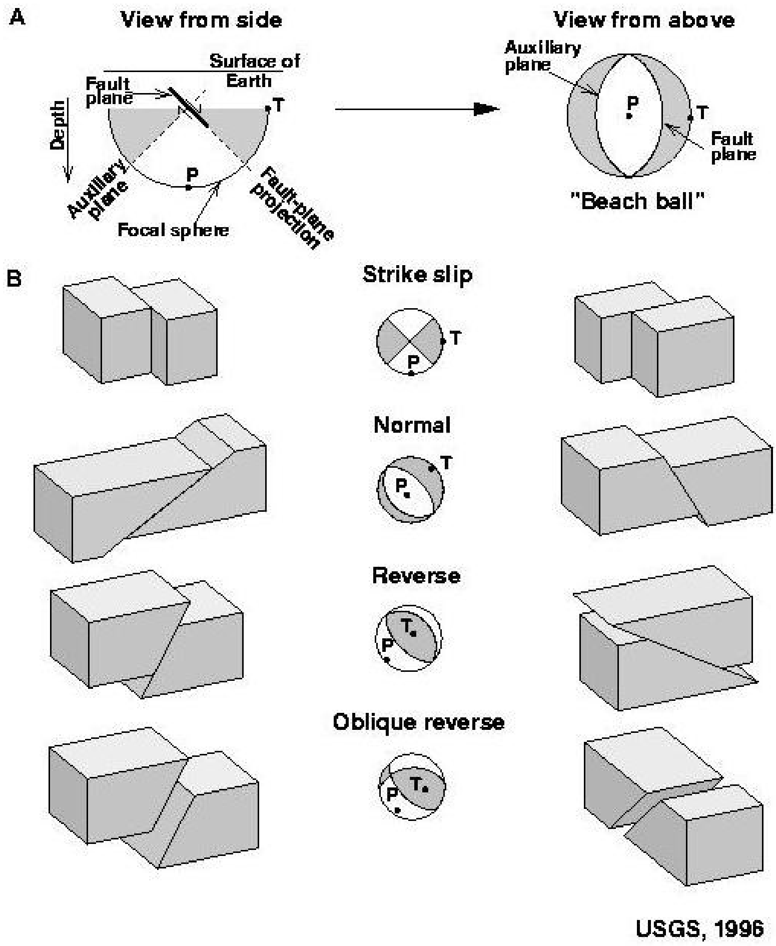


Fig. 4 – Ambiguity in identifying the fault plane in four examples.
The block diagrams adjacent to each focal mechanism are given (USGS, 1996).

The ambiguity may sometimes be resolved by comparing the two fault-plane orientations to the alignment of small earthquakes (Po Chen *et al.*, 2010), aftershocks (Peter *et al.*, 2003) or stress inversions (Martinez-Gazon *et al.*, 2016). The first three examples in Fig. 4 describe fault motion that is purely horizontal (strike slip) or vertical (normal or reverse). The oblique-reverse mechanism illustrates that slip may also have components of horizontal and vertical motion.

Theoretically, in the case of reverse and normal faults, the direction of lowering or lifting of a tectonic compartment can be determined by means of a clinometer. This can be the horizontal quartz pendulum or a watertube tiltmeter (Fig. 5), used in the recordings of the horizontal components of the earth tides (the case of the underground geodynamic observatories) or the periodic and non-periodic crustal deformations from any geodynamic observatories, either surface or underground.

Figure 6 is a schematic representation of how a watertube tiltmeter can detect the inclination direction of a fault plane generated by a seismic event.

From the records of two clinometers oriented in directions perpendicular to each other, the direction and inclination of a fault plane can be deduced. The resultant of the two components, usually east-west and north-south, is calculated (Fig. 7).

The information is more accurate when we have, for the same seismic event, recordings from several geodynamic observatories, as far as possible, on different tectonic compartments. We used clinometric records from the Căldăruşani geodynamic observatory and the Ursoiu and Crăciuneşti underground geodynamic observatories (Fig. 8).

The intermediate seismic events from Vrancea (Fig. 9) have the magnitude Mw $\geq 4$ (Table 1).

To understand the interpretation given by us of the records for each earthquake analyzed, we established the following convention: for positive values of the 1st order derivative, for the clinometric measurements in the east-west direction the crust is inclined to the west and, for the clinometric measurements in the north-south direction the crust is inclined to the north. The resultant vector of the tilt in the two directions is a plane with the same tilt direction with one of the focal mechanism solutions (Fig. 10).

We mention that the first value recorded by the sensor at the impact of the seismic wave recording station is taken into account when evaluating the tilt direction. The clinometric sensors record phenomena with periods of many orders of magnitude larger than the seismic ones.

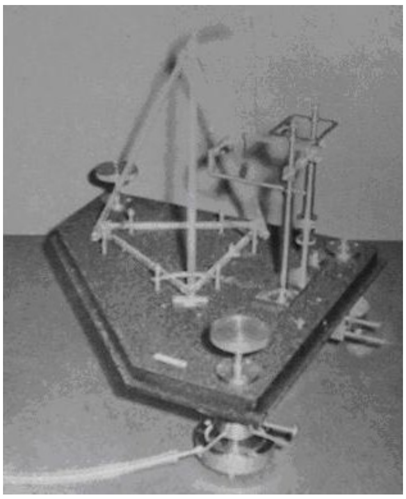

a

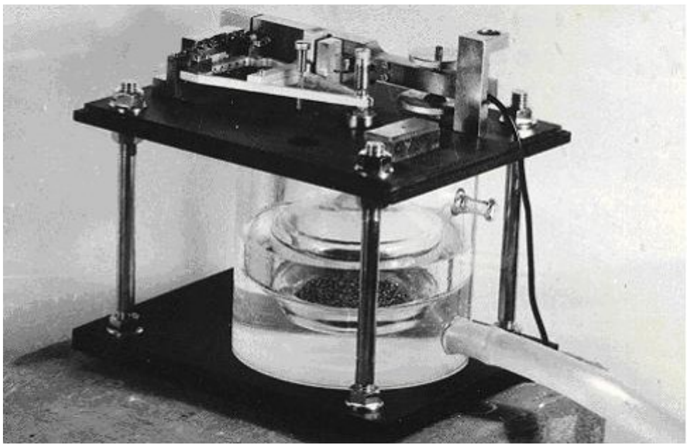

b

Fig. 5 – Horizontal quartz pendulum (a) and watertube tiltmeter (b).

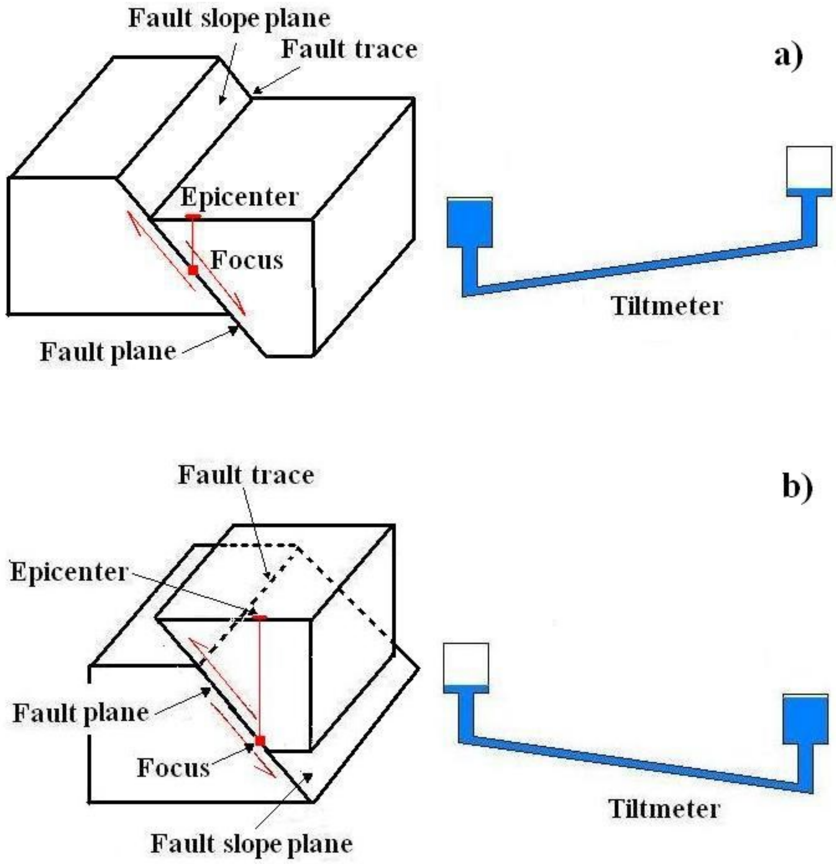


Fig. 6 – Possibility of detecting the fault plane direction with the help of a tiltmeter for a normal fault (a) and reverse fault (b).

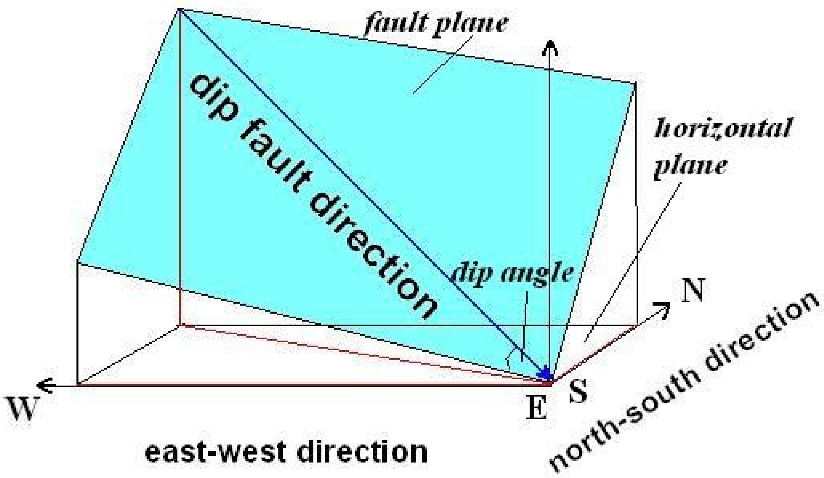


Fig. 7 – Dip fault direction from tiltmeter measurements on two perpendicular directions.

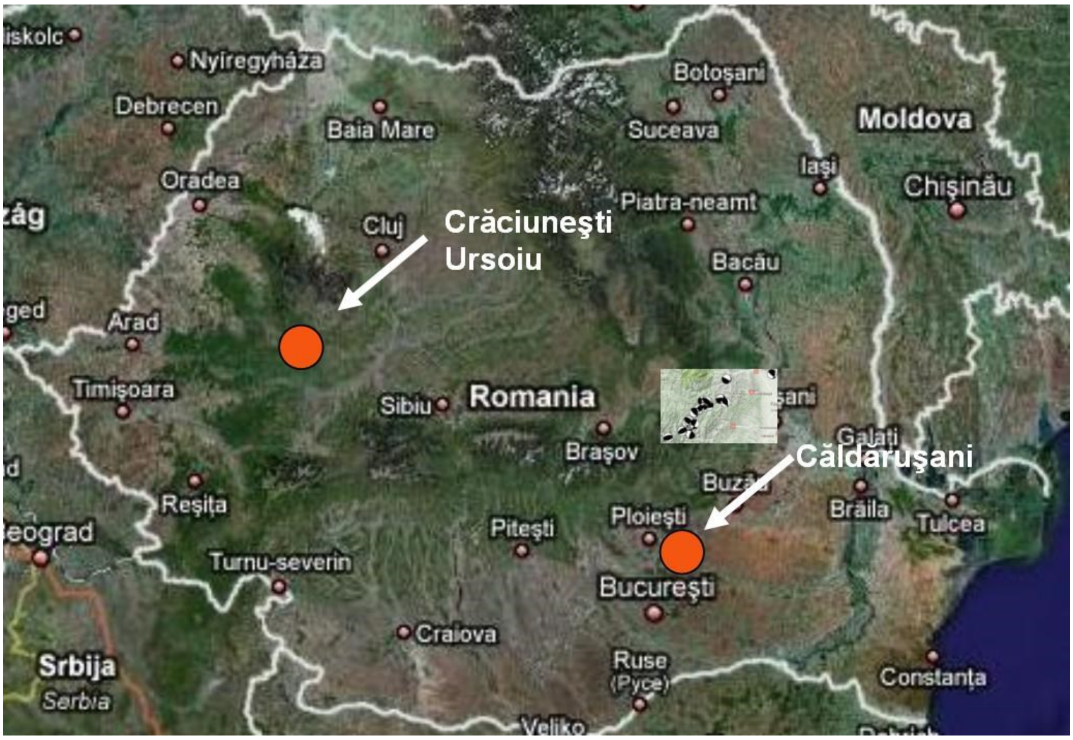


Fig. 8 – Geodynamic observatories in Romania and distribution of earthquakes analyzed in the Vrancea area.

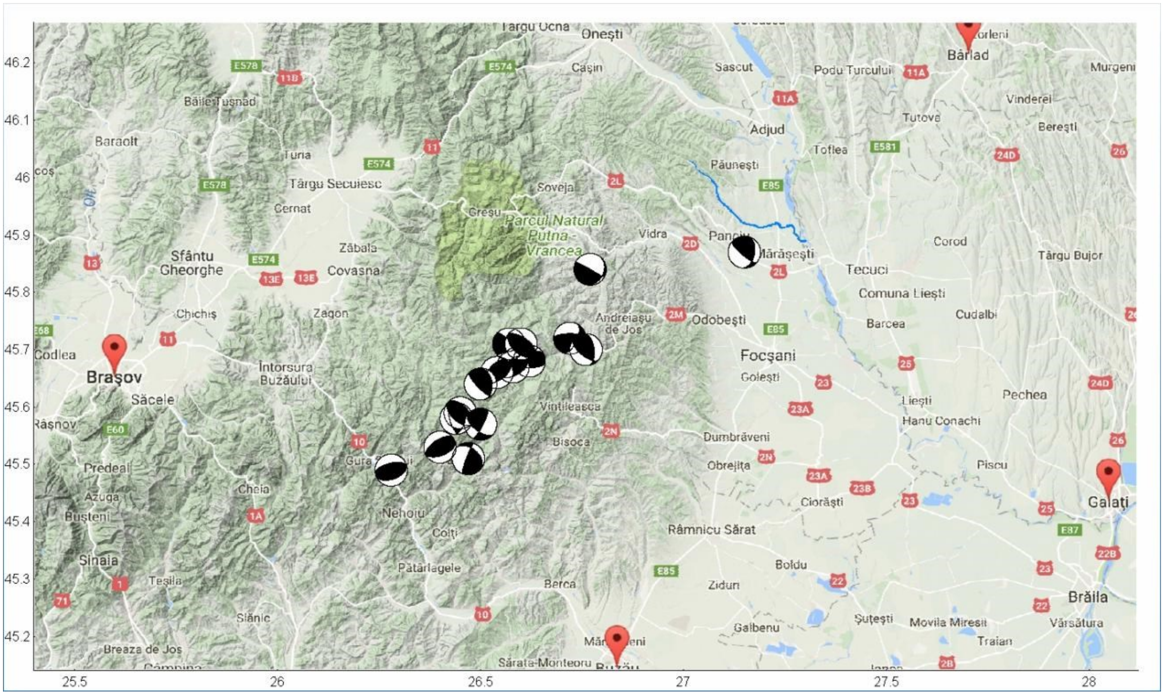


Fig. 9 – Distribution of the analyzed seismic events in Vrancea seismic zone.

*Table 1*

The intermediate seismic events from the Vrancea analyzed in this study

| Year | Month | Day | Hour | Min | Sec | Lat | Long | Depth | Mw | Strike1 | Dip1 | Rake1 | Strike2 | Dip2 | Rake2 |
|---|---|---|---|---|---|---|---|---|---|---|---|---|---|---|---|
| 2006 | 2 | 16 | 2 | 49 | 39 | 45.72 | 26.72 | 138.0 | 4.2 | 270 | 64 | 134 | 25 | 50 | 36 |
| 2009 | 4 | 25 | 17 | 18 | 48 | 45.68 | 26.62 | 109.6 | 5.4 | 249 | 39 | 71 | 93 | 53 | 105 |
| 2011 | 5 | 1 | 2 | 24 | 15.8 | 45.58 | 26.44 | 146.1 | 4.9 | 165 | 54 | 73 | 12 | 40 | 111 |
| 2013 | 10 | 6 | 1 | 37 | 21.3 | 45.67 | 26.58 | 135.1 | 5.2 | 61 | 41 | 97 | 232 | 49 | 84 |
| 2014 | 3 | 26 | 19 | 46 | 28.91 | 45.6578 | 26.5406 | 133.3 | 4.2 | 56 | 46 | 101 | 220 | 45 | 79 |
| 2015 | 1 | 24 | 7 | 55 | 47.31 | 45.7123 | 26.5712 | 88.4 | 4.3 | 314 | 74 | 153 | 52 | 65 | 18 |
| 2015 | 3 | 16 | 15 | 49 | 49.14 | 45.5991 | 26.4484 | 118.2 | 4.3 | 133 | 41 | 89 | 315 | 49 | 91 |
| 2016 | 10 | 31 | 11 | 59 | 49.76 | 45.8425 | 26.776 | 90.8 | 4 | 300 | 90 | 104 | 30 | 14 | 0 |
| 2016 | 11 | 19 | 11 | 30 | 39.22 | 45.6411 | 26.5083 | 140.8 | 4.1 | 137 | 69 | 76 | 351 | 25 | 121 |
| 2016 | 12 | 27 | 23 | 20 | 55.96 | 45.714 | 26.599 | 96.6 | 4.9 | 135 | 38 | 99 | 304 | 53 | 83 |
| 2017 | 2 | 8 | 15 | 8 | 20 | 45.49 | 26.28 | 127 | 4.5 | 256 | 51 | 94 | 70 | 39 | 85 |
| 2017 | 5 | 3 | 5 | 59 | 35 | 45.57 | 26.5 | 134 | 4.2 | 128 | 51 | 17 | 27 | 77 | 139 |
| 2017 | 5 | 19 | 20 | 2 | 44 | 45.7 | 26.76 | 118 | 4.3 | 129 | 54 | 61 | 352 | 45 | 123 |
| 2017 | 8 | 1 | 10 | 27 | 51.03 | 45.5146 | 26.4681 | 96.6 | 4.4 | 201 | 79 | 119 | 311 | 31 | 23 |
| 2017 | 8 | 2 | 2 | 32 | 12.68 | 45.5267 | 26.4014 | 132.5 | 4.9 | 236 | 48 | 82 | 68 | 43 | 99 |

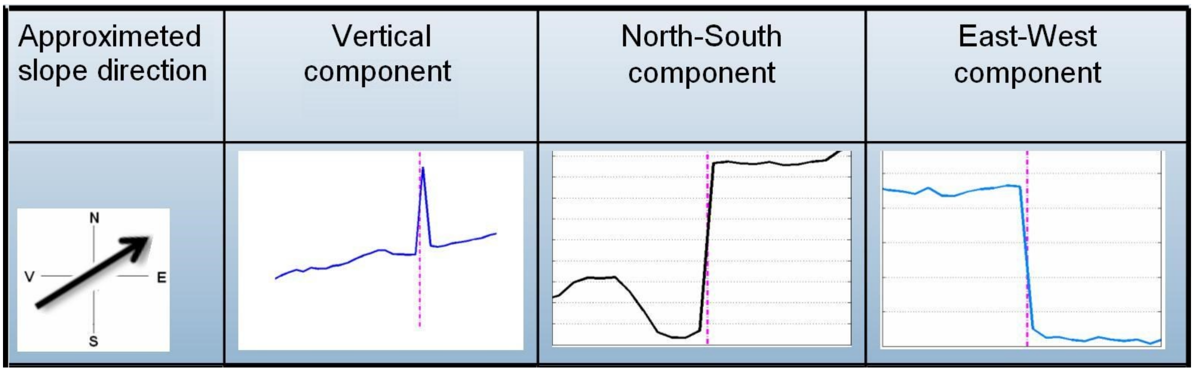


Fig. 10 – Empirical analysis of clinometric records.

In addition to the graphs corresponding to the east-west and north-south horizontal components of the tides, we used those of the gravimetric tides obtained from the processing of the data recorded using the Askania gravimeters. These behave like seismographs indicating the moment when P reaches the level of the earthtide recording station.

## 3. CASE STUDIES AND DISCUSSION

To exemplify the applied methodology we chose four intermediate seismic events with $M \geq 4$ (Table 2). In this study our evaluation is empirical only. Comparing the dip of the fault with the slope given by the clinometric measurements implies a more rigorous discussion.

*Table 2*

The intermediate seismic events chosen as case studies

| Year | Month | Day | Hour | Min | Sec | Lat | Long | Depth | Mw | Strike1 | Dip1 | Rake1 | Strike2 | Dip2 | Rake2 |
|---|---|---|---|---|---|---|---|---|---|---|---|---|---|---|---|
| 2009 | 4 | 25 | 17 | 18 | 48 | 45.68 | 26.62 | 109.6 | 5.4 | 249 | 39 | 71 | 93 | 53 | 105 |
| 2014 | 3 | 26 | 19 | 46 | 28.91 | 45.6578 | 26.5406 | 133.3 | 4.2 | 56 | 46 | 101 | 220 | 45 | 79 |
| 2015 | 1 | 24 | 7 | 55 | 47.31 | 45.7123 | 26.5712 | 88.4 | 4.3 | 314 | 74 | 153 | 52 | 65 | 18 |
| 2017 | 8 | 2 | 2 | 32 | 12.68 | 45.5267 | 26.4014 | 132.5 | 4.9 | 236 | 48 | 82 | 68 | 43 | 99 |

Figure 11 contains a summary of the results obtained. For each seismic event analyzed (Table 2), Figure 11 shows the response of gravimeters, proportional to the vertical component of the crustal deformations, and clinometers (the E-V and N-S components of the crust inclination). Combining the two clinometric components, north-south and east-west, we approximate the inclination direction of the plane of the fault. The projection perpendicular of this direction in the horizontal plane is parallel to one of the two fault plane directions. The azimuth of this perpendicular can be calculated using the values of the two clinometer tilt components. The azimuth value should be equal to or close to one of the two directions of the focal mechanism.

The solution proposed by our method is marked with a question mark on the stereographic projection. We chose the question mark because we believe that the solution chosen by us in this phase of the study should be additional validated. With a sufficient number of confirmations, it can be accepted as a standalone method.

In Figure 11a, our method agrees to the solution of the plane with the strike angle ($\varphi$) of 249 degrees and the dip angle ($\delta$) of 39 degrees because the resultant vector of the two components of the tilt is oriented towards SE, with the NS component higher than EV. Accordingly, perpendicular to this direction will be oriented to the SV. This corresponds to the above case.

In the same way, we analyze the seismic events in Fig. 11b ($\varphi = 220^{\circ}$ and $\delta = 45^{\circ}$), Fig. 11c ($\varphi = 52^{\circ}$ and $\delta = 65^{\circ}$), and Fig. 11d ($\varphi = 256^{\circ}$ and $\delta = 51^{\circ}$).

In Figures 11 (b), (c) and (d) we have no inclination signal on any measuring instrument at the underground observatories Crăciuneşti and Ursoiu. From the analysis of all the seismic events included in Table 2, it would seem that the sensors of these observatories are sensitive to fault sliding in the east-west direction (Fig. 11a) only. It is not just about the different distances between the geodynamic observatories and the Vrancea seismic zone. It is another type of seismic wave interaction with an area located on a specific tectonic alignment, in the region being present the South-Transylvanian and Brad – Săcărâmb transcrustal faults, with E–W and respectively NW–SE and intense volcanic and metallogenetic activity from the Miocene.

From this perspective, in this area no connection can be established between the inclination direction of the seismic fault plane and that obtained from the clinometric measurements. But these records can provide information about the slip direction (the rake) on the fault plane in case of an important component in the E–W direction.

## 4. CONCLUSIONS

Our proposal was to use clinometric records on two north-south and east-west directions in order to eliminate the ambiguity of the solution of the fault plane. We analysed fifteen major seismic events from Vrancea occurred between 2006 and 2017.

To exemplify, in this article we have detailed our approach for four of the fifteen earthquakes analyzed. When the recorded signal indicated an inclination of the area in which the geodynamic observatory is located, we compared the inclination direction deduced from the records with the solution of the focal mechanism. In this way we can choose one of the two possibilities of the fault plane solution.

The recordings of slow deformation of the terrestrial crust, with high sensitivity equipment, can bring additional geophysical information in eliminating the ambiguity of the fault plane solution.

But, we must take in account that:

– interpretation of the plots implies a more in-depth study of the problem, based on local and regional geology and tectonic elements;
– several geodynamic recording stations equipped with clinometric sensors of different types and continuous operation are required;
– an acceptable working algorithm requires a larger number of seismic events with known focal mechanism solution and confirmed by at least three internationally recognized sources.

We consider that our method represents a possibility to eliminate the ambiguity of the solution of the fault plane for the intermediate seismic events in Vrancea.

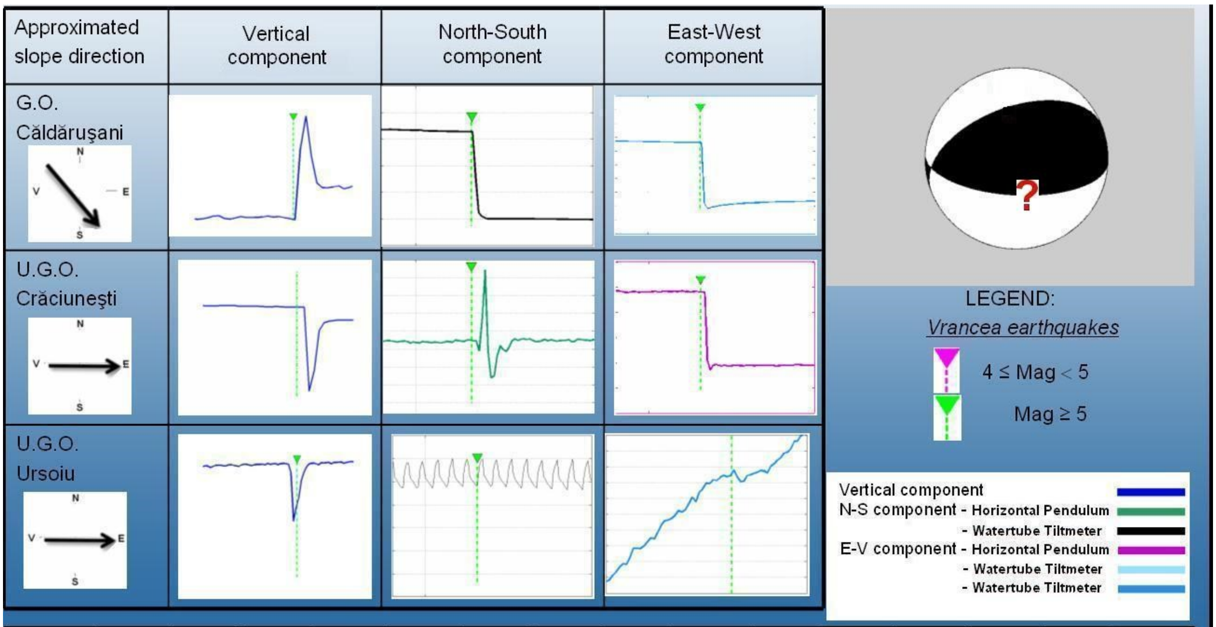


| Year | Month | Day | Hour | Min | Sec | Lat | Long | Deep (Km) | Mag | Strike1 | Dip1 | Rake1 | Strike2 | Dip2 | Rake2 |
|---|---|---|---|---|---|---|---|---|---|---|---|---|---|---|---|
| 2009 | 4 | 25 | 17 | 18 | 48 | 45.68 | 26.62 | 109.6 | 5.4 | 249 | 39 | 71 | 93 | 53 | 105 |

**(a)**

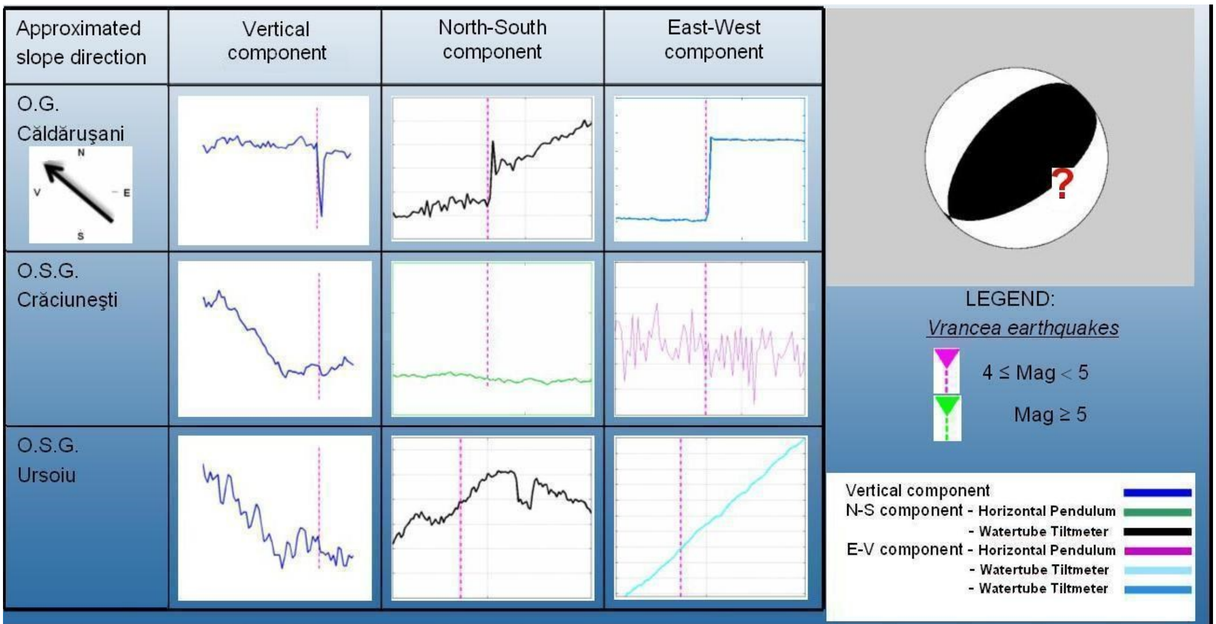


| Year | Month | Day | Hour | Min | Sec | Lat | Long | Deep (Km) | Mag | Strike1 | Dip1 | Rake1 | Strike2 | Dip2 | Rake2 |
|---|---|---|---|---|---|---|---|---|---|---|---|---|---|---|---|
| 2014 | 3 | 26 | 19 | 46 | 28.91 | 45.657 | 26.540 | 133.3 | 4.2 | 56 | 46 | 101 | 220 | 45 | 79 |

**(b)**

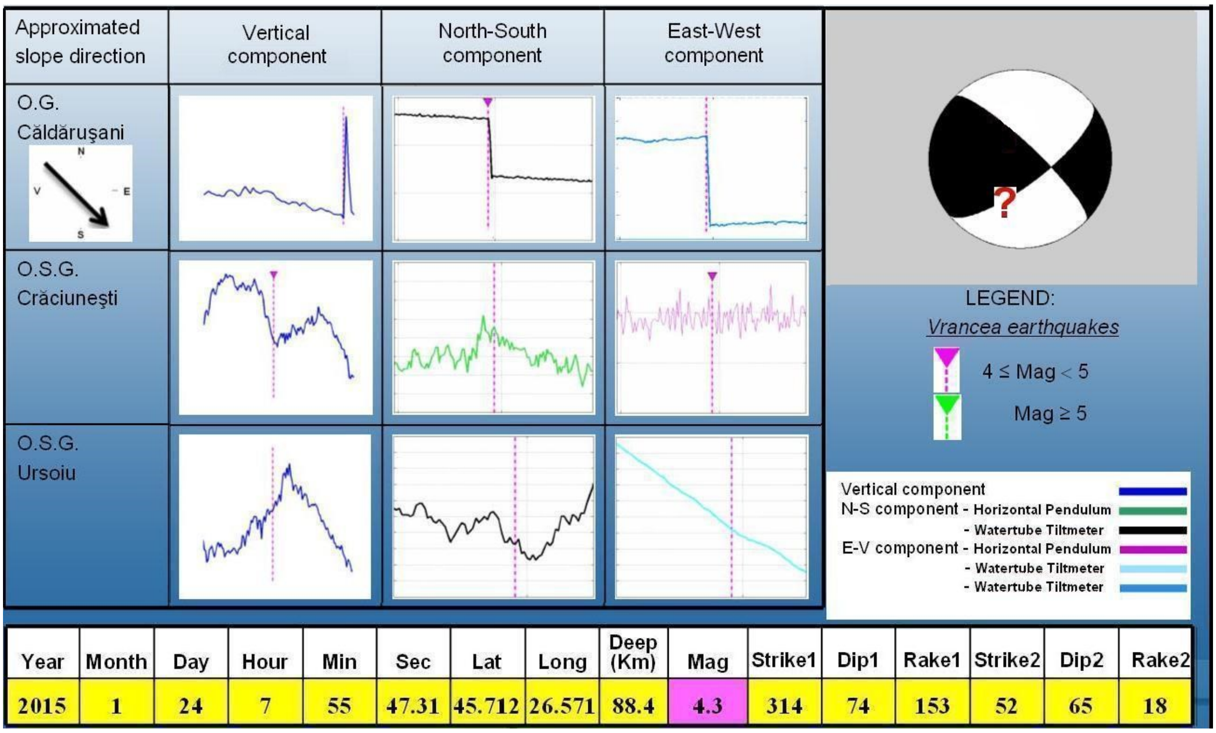


**(c)**

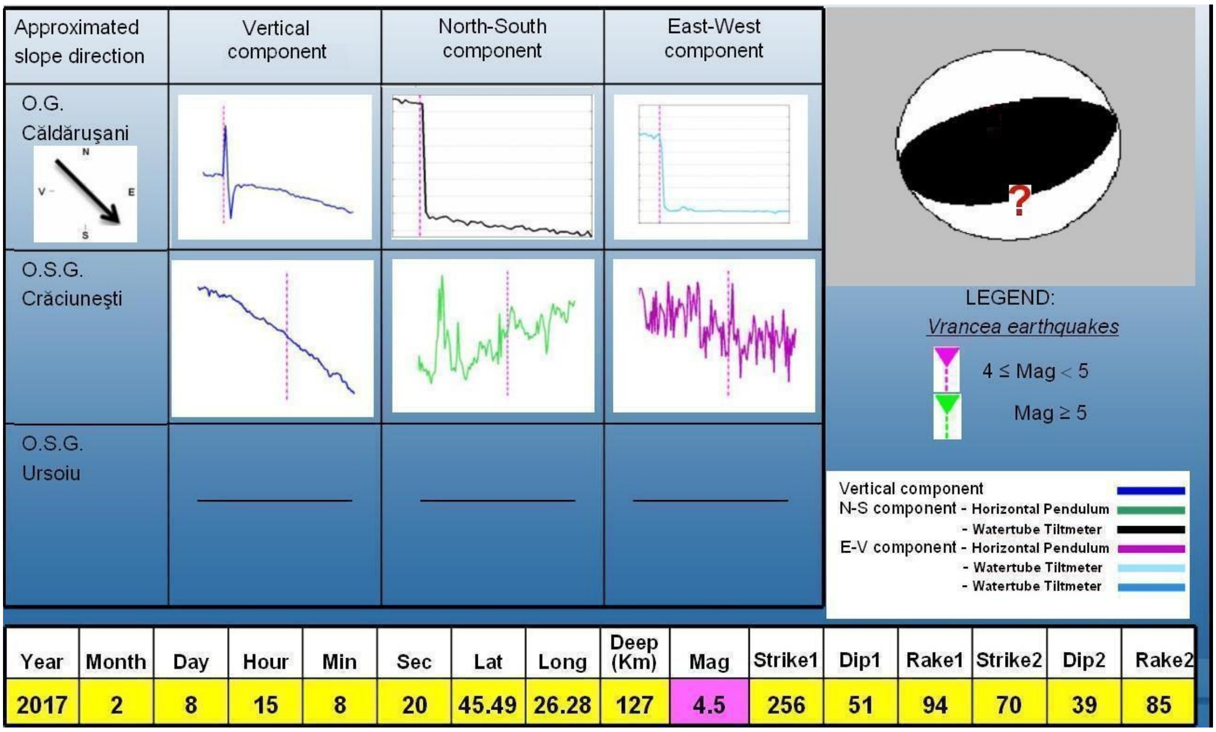


**(d)**

Fig. 11 – Slope direction approximated in the case of four earthquakes from Vrancea.

REFERENCES

BATH, M. (1979), *Introduction to Seismology*, Birkhauser Basel Publisher, ISBN 978-3-0348-5285-2, 428 pp.

HAVSKOV, J., OTTEMÖLLER, L. (2010), *Routine Data Processing in Earthquake Seismology*, 347 pp., Springer.

MARSHALL, S.T. (2010), *Introduction to Geophysics, Chapter 5, Earthquakes and Seismotectonics*. https://www.appstate.edu/~marshallst/GLY3160/lectures.html.

MARTÍNEZ-GARZÓN, P., BEN-ZION, Y., ABOLFATHIAN, N., KWIATEK, G., BOHNHOFF, M. (2016), *A refined methodology for stress inversions of earthquake focal mechanisms*. J. Geoph. Res. (Solid Earth), **121**, Issue **12**, 8666-8687 pp., https://doi.org/10.1002/2016JB013493.

SHEARER, P.M., HARDEBECK, J.L., ASTIZ, L., RICHARDS-DINGE, K. B. (2003), *Analysis of similar event clusters in aftershocks of the 1994 Northridge, California, earthquake.* J. Geophys. Res. (Solid Earth), **108**, No. **B1**, CiteID 2035, doi:10.1029/2001JB000685.

PO CHEN, THOMAS, H.J., LI ZHAO (2010), *Resolving fault plane ambiguity for small earthquakes.* Geophys. J. Int., **181**, 493–501doi: 10.1111/j.1365-246X.2010.04515.x

STEIN, S., WYSESSION, M. (2003), *An Introduction to Seismology, Earthquakes and Earth Structure*, Blackwell Publishing Ltd., 490 pp.

YAN, Y.K., DAVID, D.J. (1998), *Spatial aftershock distribution: Effect of normal stress.* J. Geophys. Res., **103**, no. **B10**, pp. 24, 453–24, 467, October 10, 1998.

*Received: August 7, 2018*
*Accepted for publication: November 12, 2018*